Synthesis of Novel All-Dielectric Grating Filters Using Genetic Algorithms

Cinzia Zuffada, *Senior Member, IEEE,* Tom Cwik, *Senior Member, IEEE,* and Christopher Ditchman

***Abstract*—The feasibility of novel all-dielectric waveguide grating filters is demonstrated, using a genetic algorithm (GA) to solve for material dielectric constants and geometric boundaries separating homogeneous regions of the periodic cell. In particular, GA's show that simple geometries (not previously reported) utilizing a small number of layers and/or gratings can be found to yield bandpass or stop-band filters with user defined linewidth. The evaluation of the fitness of a candidate design entails the solution of an integral equation for the electric field in the cell using the method of moments (MoM). Our implementation is made efficient by using only very few design frequency points and accurately approximating a given filter transfer function by a quotient of polynomials as a function of frequency. Additionally, the problem impedance matrices are conveniently represented as the product of a material independent matrix and a vector of dielectric constants, thus allowing us to fill the matrices only once. Our code has been parallelized for the Cray T3D to take advantage of the intrinsic parallelization efficiencies offered by GA's. Solutions are illustrated for a very narrow-band single-grating transmission filter and a relatively broad-band double grating reflection filter. Additionally, a solution for a five homogeneous layers Fabry–Perot filter is also presented.**

***Index Terms*—Filters, genetic algorithms.**

I. Introduction

THIS work is concerned with the synthesis of inhomogeneous all-dielectric (lossless) periodic structures that act as filters. The design of electromagnetic components, in general, involves finding the values of the relevant parameters, which ensure that the structure performs in accordance with specified design criteria. The particular type of design described here can be thought of as an inverse-source problem since it entails finding a distribution of sources that produce fields (or quantities derived from them) of given characteristics. Electromagnetic sources (electric and magnetic current densities) in a volume are related to the outside fields by a well-known linear integral equation. Additionally, the sources are related to the fields inside the volume by a constitutive equation involving the material properties. Then, the relationship linking the fields outside the source region to those inside is nonlinear in terms of material properties such as permittivity, permeability, and conductivity. Dielectric filters made as stacks of inhomogeneous gratings and layers of materials have been used in optical technology for some time, but are not common at microwave frequencies. The problem is then finding the periodic cells geometric configuration and permittivity values that correspond to a specified reflectivity/transmittivity response.

This type of design problem shares some of the formalism with that of the identification/location of dielectric objects given their scattered fields in that they are both nonlinear inverse problems described by the same integral equations. Some approaches to solving the reconstruction problem have been proposed [1], [2], which suggest a useful strategy also applicable in part to the design case. Specifically, the solution of the nonlinear inverse problem is cast as a combination of two linear steps by explicitly introducing the electromagnetic sources in the computational volume as a set of unknowns in addition to the material unknowns. This allows to solve for material parameters and electric fields in the source volume which are consistent with Maxwell's equations. Solutions are obtained iteratively by either decoupling the two steps in [1] or by keeping them coupled in [2]. Irrespective of the specific solution method, this approach involves a potentially large number of unknowns, particularly when many frequencies/illumination angles are of interest, which is the case in design. In order to reduce the number of unknowns or the complexity of the operators, we introduce a simplification in the iterative scheme by first inverting for the permittivity only in the minimization of a cost function and, then, given the materials, by finding the corresponding electric fields through direct solution of the integral equation in the source volume. The sources thus computed are used to generate the far fields and the synthesized filter response. The cost function is obtained by calculating the deviation between the synthesized value of reflectivity/transmittivity and the desired one. Solution geometries for the periodic cell are sought as gratings (ensembles of columns of different heights and/or widths) or combinations of homogeneous layers of different dielectric materials and gratings. Hence, the explicit unknowns of the inversion step are the material permittivities and the relative geometric boundaries separating homogeneous parcels of the periodic cell.

The inversion step to compute materials and geometric boundaries is performed using the genetic algorithm (GA) package PGAPACK [3]. The choice of a GA was suggested by the primary objective of this work, i.e., investigating the feasibility of dielectric waveguide filters whose geometry is simpler or smaller or more easily manufacturable than existing designs and understanding the trends in required numbers, values of materials, and their geometric configurations as

Manuscript received March 19, 1997; revised November 11, 1997. This work was performed at the Jet Propulsion Laboratory under Contract with the National Aeronautics and Space Administration.

The authors are with the Jet Propulsion Laboratory, California Institute of Technology, Pasadena, CA 91109 USA.

Publisher Item Identifier S 0018-926X(98)03373-0.

functions of the prescribed filter response. To this end, several advantages are offered by global optimization techniques such as GA's over local gradient-based optimization methods used with nonlinear problems for electromagnetic designs where the solution space has many extrema. In particular, the ability of GA's to sample a given parameter space globally not only avoids the common pitfalls of local minimization algorithms, but holds the promise of finding novel solutions perhaps not thought to exist. Some applications reported in the literature include the design of thinned phased-arrays [4], of multilayer radar absorbers [5], of multilayer optical filters [6], of loaded antennas [7], [8], and of monolithic microwave integrated circuits (MMIC) component shapes [9]. Finally, the specific choice of PGAPACK was suggested by its availability as a parallel and portable library, thus affording an efficient use of a versatile software tool.

It has been remarked that GA's carry a considerable computational cost. Naturally, the most expensive part of the computational cycle is the forward module that performs the evaluation of a candidate solution to determine its fitness. In our case, this consists of solving a set of integral equations for the electric fields in the cell, one for each design frequency/illumination angle. Although the impedance matrix depends on the solution vector of materials and boundaries candidates, it can be formed as a product of a solution-independent matrix and a vector. This procedure allows us to fill the set of frequency-dependent impedance matrices only once. Additionally, the number of design frequencies at which the integral equations are actually solved is a small set of values within the frequency range of the desired filter response. The reduction is afforded by approximating the desired filter response by a quotient of frequency dependent polynomials, through the procedure of transfer function parameter estimation described in [10]. Furthermore, full advantage has been taken of the parallel implementation of PGAPACK for the Cray T3D. The parallelization scheme used for the GA is an intuitive, simple, master-slave configuration, where the expensive evaluation cycles are distributed among the processors.

Section II describes the electromagnetic scattering from a two-dimensional (2-D) inhomogeneous dielectric periodic structure, which constitutes the "forward module" of our inversion scheme. Section III highlights some of the relevant features of the specific GA solver used in our work. Section IV focuses on the design of dielectric waveguide-grating filters and emphasizes the role of our inverse approach in finding novel solutions. Section V presents and discusses numerical results for three different types of filters designed with our code.

II. Formulation of the Forward Scattering from a Dielectric Grating

At every step, we evaluate the scattering from a candidate solution for a dielectric grating according to the formulation described in the following. Fig. 1(a) shows the geometry of a dielectric grating, periodic in the x dimension with period T_x, infinite in y, and having a thickness $t(x)$ variable over the cell. The cell material is characterized by complex permittivity and permeability. The polarization with the electric field parallel to the strip will be considered (E polarization); a formulation for the perpendicular polarization can be similarly developed. To properly pose the scattering problem for a periodic structure, the excitation field must be a function with constant amplitude and linear phase. The incident field is defined as [11]

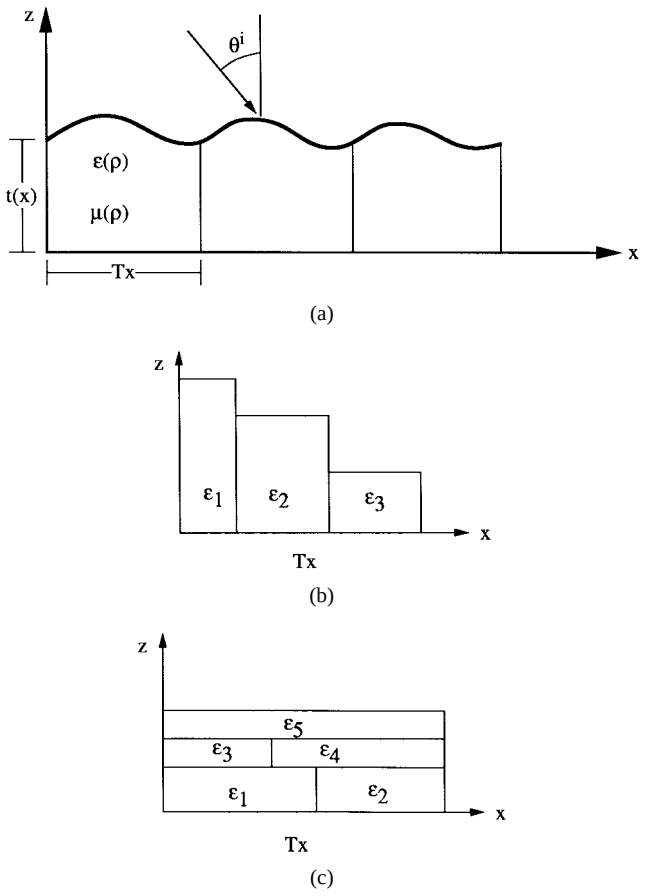

Fig. 1(a). Geometry of a 2-D periodic structure showing an inhomogeneous dielectric cell and the illuminating plane wave. (b) and (c) Specific cell geometries realizable with our methodology.

$$E^i(x,z) = E_0 \psi_0(x)\, e^{j k_{z_0} z} \tag{1}$$

where

$$\psi_m(x) = \frac{1}{\sqrt{T_x}}\, e^{j k_{x_m} x} \tag{2}$$

and

$$k_{x_m} = \frac{2\pi}{T_x} m + k_{x_0}, \quad k_{x_0} = k \sin\theta^i$$

$$k_{z_m} = \begin{cases} \sqrt{k^2 - k_{x_m^2}}, & k \geq k_{x_m} \\ -j\sqrt{k_{x_m^2} - k^2}, & k \leq k_{x_m} \end{cases}$$

and the $e^{j\omega t}$ time convention is used. Using the electric field integral equation, the unknown induced current $J(\rho)$ is found at each design frequency/illumination angle from

$$E^i(\rho) = \frac{1}{j\omega\varepsilon_0 \chi(\rho)} J(\rho) - E^s(\rho) \tag{3}$$

where all components are y directed, and χ is the contrast function

$$\chi(\rho) = \varepsilon_r(\rho) - 1.$$

The scattered field is found from integrating the induced currents over the grating

$$E^s(x,z) = \frac{-\omega}{4}\int_0^{T_x}\int_0^{t(x)} \mu(x',z')J(x',z') \times G_p(x,z \mid x',z')\,dx',dz' \tag{4}$$

where

$$G_p(x,z \mid x',z') = \frac{1}{4j}\sum_{m=-\infty}^{\infty} H_0^{(2)}\big(k\sqrt{(x-x'-mT_x)^2+(z-z')^2}\big) \times e^{jk_{x_0}mT_x}$$

is the 2-D periodic Green's function—the outgoing Hankel function of order zero—representing the field due to source points within each cell [12]. Using this periodic spatial Green's function, the integration area is then over one periodic cell. Equation (4) contains an integrable singularity, occurring as the source and observation points are made to coincide. The Appendix outlines a method for isolating this singular point and performing the integration in an efficient manner. The result is

$$E^s(x,z) = \int_0^{T_x} dx' \int_0^{t(x)} dz'\,J(x',z')\big[Z_m^P(x,z \mid x',z') - Z_m^P(x,z \mid x',z'+\delta)\big] + \sum_m \tilde{Z}_m \tilde{I}_m^{\pm}\psi_m(x)\,e^{\mp k_{z_m}(z+\delta)} \tag{5}$$

where the various terms are defined in the Appendix.

The method of moments (MoM) is used to solve the above integral equation. The numerical solution of (3) is found by first discretizing the current over a periodic cell in a pulse basis set

$$J(x,z) = \sum_{p'=1}^{P}\sum_{q'=1}^{Q} C_{p'q'}\pi_{p'}(x)\pi_{q'}(z), \quad P_x'Q' = P'Q' \tag{6}$$

where the pulse is defined as

$$\pi_p(u) = \begin{cases} 1, & (p-1)\Delta u < u < p\Delta u \\ 0, & \text{elsewhere.} \end{cases}$$

In our MoM procedure, point matching is used with the testing functions being

$$T_{pq}(x,z) = \delta\left[x-\left(p-\frac{1}{2}\right)\Delta x\right]\delta\left[z-\left(q-\frac{1}{2}\right)\Delta z\right]. \tag{7}$$

The matrix system for the unknown coefficients C is then

$$\langle E^i, T_{pq}\rangle = \sum_{p'q'} C_{p'q'}\left\langle \frac{1}{j\omega\varepsilon_0\chi}\pi_{p'}\pi_{q'}, T_{pq}\right\rangle - \sum_{p'q'}[\langle E^{ss}(x,z), T_{pq}\rangle + \langle E^{sn}(x,z), T_{pq}\rangle] \qquad pq = 1,2,\ldots P'Q' \tag{8}$$

where the inner product is defined as

$$\langle f,g\rangle = \int_0^{T_x} dx \int_0^{t(x)} dz\, fg^*.$$

The matrix of (8) depends on the materials through the contrast χ. However, it can be represented as a product of a material-independent matrix times the vector of the contrasts at each discretization cell. Therefore, the basic matrix is filled only once for each design frequency and it is simply updated at each iteration step by multiplication with the current vector of contrasts. It seems that there is one independent contrast value for each discretization cell used in our MoM. In reality, we constrain the grating periodic cell to be composed of a number of regions with different materials, separated by boundaries, and arranged in a combination of homogeneous horizontal layers and/or strips with χ varying along the x and z directions, as illustrated in Fig. 1(b) and (c). Then the set of inversion parameters for the GA, i.e., the different values for χ and boundary locations along x and z, is much smaller than the number of discretization cells. A mapping algorithm transforms this reduced parameter set for a candidate solution to the full vector of contrasts at each discretization cell.

Assuming that only the dominant $(m = 0)$ mode is propagating, the reflection and transmission coefficients are found from evaluating the total field at $z \gg t$ and $z \ll 0$, respectively

$$R = \frac{-\omega}{4E_0}\frac{1}{2jk_{z_0}}\int_0^{t(x)} dz'\mu\tilde{J}_0(z')\,e^{jk_{z_0}z'} \tag{9a}$$

$$T = 1 - \frac{\omega}{4E_0}\frac{1}{2jk_{z_0}}\int_0^{t(x)} dz'\mu\tilde{J}_0(z')\,e^{-jk_{z_0}z'} \tag{9b}$$

where the transform of the current is given in the Appendix.

In designing a filter the desired behavior of R and T (RR^* or TT^*) within a continuous range of frequencies is often specified; since the coefficients of the current are frequency dependent, it would appear that to evaluate the response of a candidate many MoM solutions of (5) must be calculated. However, any prescribed filter response must satisfy the condition of realizability. It is well known from classical lumped parameter filter design that realizability requires that the insertion loss (as a function of frequency) be representabable as the ratio of two polynomials of even powers of frequency. Then the problem is reduced to representing the desired filter response by a quotient of polynomials working with a set of prescribed values sufficient to determine the unknown coefficients. As discussed in [10], the general representation for a magnitude-squared network transfer function with poles and zeroes is given by

$$|F(\omega_i)|^2 = \frac{\sum_{j=0}^{N-1} B_j(\omega_i)^{2j}}{\sum_{j=0}^{N} A_j(\omega_i)^{2j}} + \sum_{j=0}^{K} C_j(\omega_i)^{2j} \tag{10}$$

where the quantity on the left-hand-side is either RR^* or TT^*. Equation (10) can easily be turned into a system of equations in the $2\times N+K$ unknowns A_j,B_j, and C_j. Hence, the solution of (5) is calculated only at $2\times N + K$ design frequencies and the correspondent values for (9a) or (9b) are used to solve for (10). The polynomial approximation of (9a) or (9b) are then obtained at all frequencies of interest and used in the evaluation of the residual. In our implementation we investigated prescribed insertion loss functions, which can be represented very well by (10), and in the case of a Butterworth response discussed in Section VI, exactly. Naturally, the frequency response of a distributed system might not be consistent with (10) and a thorough investigation of its applicability is beyond the scope of this work. However, since

we are concerned with filter designs in the neighborhood of one resonance, it is expected that (10) will apply approximately to the filter transmittivity and/or reflectivity. Indeed, for our filters we verified *a posteriori* that the solutions calculated by extrapolation from (10) were in agreement with those calculated directly.

III. PGAPACK Parallel Genetic Algorithm

The general properties of GA's are described very extensively in the literature (see, for example, [13]) and here we summarize only the most important features of the specific library used in our work. PGAPACK is a parallel GA library developed at Argonne National Laboratory by Levine [3]. Both serial and parallel versions are available for a large number of computer systems (including the Cray T3D) using message passage interface (MPI) system libraries. The low-level routines are written in C, but interface (wrappers) routines are available which allow PGAPACK to be used in a FORTRAN code. For simple problems, or limited user involvement, a single high-level call to the library is available. More user control can be achieved by calling the GA lower level functions explicitly in which case many parameters affecting the mechanisms of selection, recombination, and fitness evaluation can be adjusted. We have chosen a flexible, customized usage in our work, which included writing some additional low-level routines. Several data types are admissible to represent the string of unknowns called "gene"; we have chosen real encoding whereby each unknown is represented by one real number whose value can vary continuosly within a predefined range. Hence, the solutions are not limited to the discrete approximations associated with a binary representation. We find PGAPACK implementation of real encoding very appealing also because the meaning of the operations of crossover and mutation are more transparent and, we believe, more effective than for binary encoding. To illustrate the point on a simple example, we have simulated the application of a crossover and a mutation operations to a real encoded gene contrasted to a binary encoded gene in Fig. 2. (Note that the two representations are not meant to describe the same numbers.) It is assumed that there are four variables and that three bits have been chosen to represent each of them in the binary approximation; by contrast a full real number is used to represent an allele in real encoded genes. A two-point crossover has been chosen in both cases. In either case, the crossover operation generates new strings by combining portions of two existing strings, broken at one or more points. While in a binary representation, the bit sequence representing one variable can be broken by the crossover operation at any point, as illustrated in (α) on the left of Fig. 2, in this real encoding, the full value of a variable is always preserved as seen in (α) on the right of Fig. 2. For our specific problem, we found uniform crossover to be very effective and we specified a probability of occurrence of 50%, consistent with PGAPACK author's recommendations. Crossover then simply rearranges the sequence of candidate values, and then mutation changes them. Note also that the mutation operation acquires a more versatile meaning and is not just the flipping of a bit in the string. Instead, an allele is mutated by modifying its value according to some algorithms, for example, by a percentage of the current value chosen probabilistically within a range (compare, for example, (β) on the left and right of Fig. 2). We have been using the Gaussian mutation type in our work where the allele is mutated by adding a random number obtained from a Gaussian distribution with zero mean and standard deviation prescribed by the user to be a percentage of the current allele's value. Typically, 5–10% was specified in our test runs. Larger percentages resulted in less desirable (higher residual value) solutions for the same number of generations. One can see that with this real encoding, crossover is the most important operation during the early generations, when the gross features of a good solution are evolved. Later on, mutation becomes the critical mechanism that allows the fine features of the solution to emerge. It is noted that PGAPACK "swap only" crossover operator used with real encoding is not the only possible one; for example, implementations exist where arithmetic or geometric averages of the alleles values being swapped form the child strings [14]. In addition to the types of encoding described so far, PGAPACK allows the user to define custom data types, which implies writing a set of custom functions to perform the operations which are data-type dependent. This facility is very useful for problems requiring a mixed type of variable encoding.

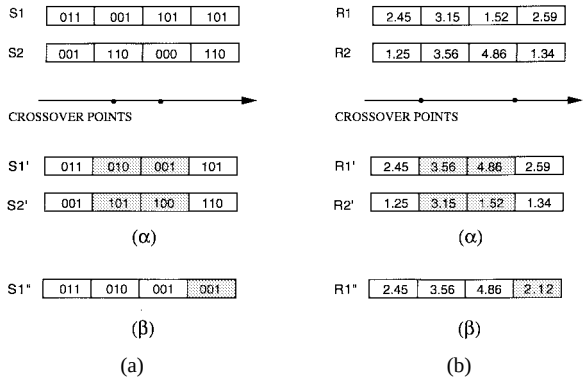

Fig. 2. Example outcome of crossover (α) and mutation (β) operations in (a) binary encoded gene versus (b) real encoded gene. In both cases, chromosome is composed of four genes. In the binary case, three bits have been chosen to represent each allele.

IV. An Application: Guided-Mode Resonance Filters

It has been demonstrated that planar dielectric layer diffraction gratings exhibit sharp resonances due to the coupling of exterior evanescent diffractive fields to the leaky modes of dielectric waveguides. In these cases, efficient switching of energy between (nearly) totally reflected zero-order mode and (nearly) totally transmitted zero-order mode is achieved with proper choice of the cell size. Such property leads to the possibility of filter designs whose arbitrarily narrow linewidths can be controlled by the choice of modulation amplitude and mode confinement. In optics, the guided-mode resonance effect has been combined with classical antireflection properties of thin film structures, leading to the design of symmetric reflection filters with low sidebands over wavelength ranges related to the number of films used and their dielectric constants [15].

Recently, a combination of guided-mode resonance and high-reflection layer design has been demontrated to yield transmission bandpass filters [16]. A reflection filter of this type has also been demonstrated in the microwave region [17]. In the present paper, we investigate the possibility of finding new types of waveguide-grating filter solutions in the microwave region. In the above studies, "forward scattering" analysis techniques were used to obtain the filter response, starting from a set of user specified filter parameters and relying on known properties of antireflection (half-wavelength) or high-reflection (quarter wavelength) homogeneous layers/gratings for reflection and transmission filters, respectively. By contrast, here we start from a desired filter response and determine the grating/layer configuration and dielectric constants of the solution, without constraining the thicknesses to be a specified fraction of the resonance wavelength. This approach is particularly appealing in the microwave region where the traditional approach used in optics would yield solutions that are too thick for practical use. At the same time, the potential reduction in size can be beneficial in optics too, since thinner filters have a wider range of application.

Some important issues can be explored with our inverse approach. The first relates to the shape of the resonance response of the filter; in particular, we have investigated the possibility of synthesizing a transmission response described by a Lorentzian lineshape with controllable linewidth to achieve a very narrow band. On the other hand, we have also searched for solutions whose reflection response follows a given Butterworth curve to demonstrate that broad-banded response and sharp cutoff are also obtainable with these type of structures. A second issue concerns the actual number and configuration of gratings/layers required; specifically, we have been looking for the "simplest" solutions, i.e., those which involve only one grating, if possible. In particular, we have also investigated the possibility of using more than two materials to make one grating to achieve symmetric responses, exhibiting a sharp resonance and low sidebands. We have seen that there is a tradeoff between the values of the dielectric constants (resulting in the modulation) and the thickness of the periodic cell. Since it is our interest to examine the possibility of designs that might not be known to exist, we have not restricted the choice of dielectric constants to a small set of familiar values, but instead have considered the materials that can, in principle, exist. Specific numerical results are presented in the following section.

V. Numerical Examples

A novel design for a narrowline bandpass filter is presented in Fig. 3. By allowing the unknown dielectric constants to span the range between one and ten—a realistic assumption in the microwave region—we have obtained a solution for a three-material single waveguide-grating transmission filter with a bandwidth of 0.7% of the central wavelength of 3 cm. The geometry of the cell and illumination condition is reported in the figure together with the obtained filter response. The grating period T_x and thickness were fixed and we solved for the two geometric boundaries (ranging between zero and

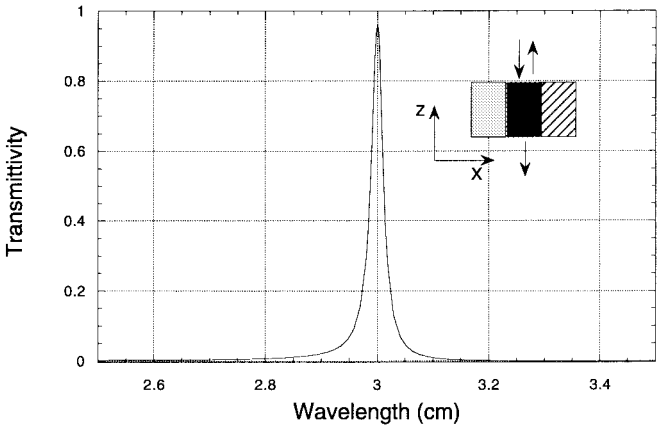

Fig. 3. Transmittivity response for three-material single-grating filter designed to satisfy a Lorentzian lineshape. Cell size is $T_x = 2.2$ cm, thickness $= 0.9$ cm. Boundary locations are at $x_{12} = 1.15$, $x_{23} = 1.78$ cm. Dielectric constants of materials from left to right are $\varepsilon_1 = 2.498$, $\varepsilon_2 = 7.939$, $\varepsilon_3 = 10$.

T_x) and three material permittivities (ranging between one and ten). The chromosome is constructed as the sequence of material parameters followed by the boundary locations. The prescribed response is a Lorentzian line approximated according to (10); for this particular case, we determined numerically that $N = 2$, $K = 1$ was sufficient to represent the Lorentzian with at least six digits of accuracy. As a result, five design wavelengths were used to specify RR^*: 2.5, 2.75, 3, 3.25, and 3.5 cm. The residual was actually evaluated for a set of 103 wavelengths not equally distributed in the range 2.5–3.5 cm, but rather having a denser distribution in a small region around the expected resonance (21 points in the range 2.98–3.02 cm). We took the population size to be 3000 with replacement through crossover and mutation of up to 300 (steady state) at every generation and performed the calculations on the JPL Cray T3D. Gridding the cell with 21 $\times$ 7 points was sufficient to achieve convergence to the solution reported in the figure in about 150 iterations. For each iteration, the overall cost of replacement, i.e., the time necessary to evaluate the newly created strings at each iteration, was about 5 s using 64 processors.

As an example of a stopband filter, a response described by a fourth-order Butterworth polynomial with bandwith of 8% of the center wavelength was input to the GA as a prescribed reflectivity. A synthesized two-grating solution, the simplest realization with the smallest cell size which was found, is illustrated in Fig. 4 with the obtained response contrasted with the desired one. Sixteen wavelengths were specified to exactly represent the Butterworth curve according to (10) and the residual was calculated at 51 points. Both sets of points were uniformly distributed in the range of interest of 2.5–3.5 cm. The trial cell size was chosen to be 2 $\times$ 2.7 cm and was gridded with 10 $\times$ 14 points. A population size of 4000 with 10% replacement was chosen and convergence was reached in about 300 generations. The calculation was performed on the Cray T3D using 128 processors in about 1 h with a cost of replacement of about 13 s.

Finally, to validate this method for a class of structures for which there are analytical solutions, we started with the

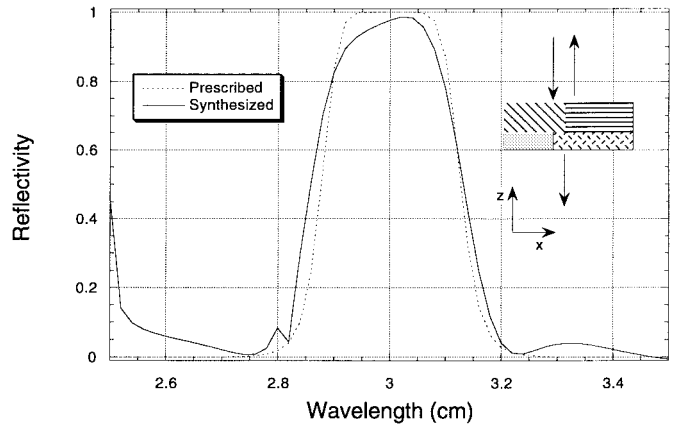

Fig. 4. Reflectivity response for double-grating filter designed to satisfy a Butterworth lineshape of the fourth order. Cell size is $T_x = 2.5$ cm, thickness $= 2.7$ cm. Boundary locations along x are at $x_{12} = 1.5$ cm (bottom grating) and $x_{34} = 1.25$ cm (top grating). Thickness of bottom grating is 0.96 cm. Dielectric constants of the four materials are $\varepsilon_1 = 1.319$, $\varepsilon_2 = 9.172$, $\varepsilon_3 = 3.638$, $\varepsilon_4 = 4.113$.

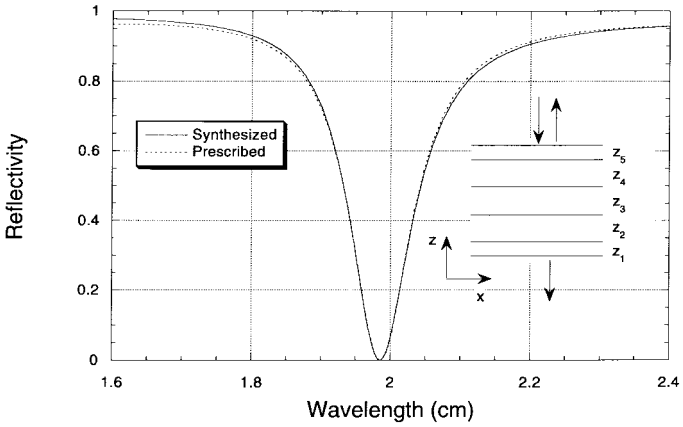

Fig. 5. Reflectivity response of five homogeneous layer filter designed to satisfy curve illustrated in the figure as "prescribed." Overall thickness of the structure is 1.62 cm. Thicknesses of each layer are (from bottom) $z_1 = 0.2$, $z_2 = 0.4$, $z_3 = 0.42$, $z_4 = 0.4$, and $z_5 = 0.2$ cm. Dielectric constants of the five materials are $\varepsilon_1 = 6.5$, $\varepsilon_2 = 1.023$, $\varepsilon_3 = 6.373$, $\varepsilon_4 = 1.067$, and $\varepsilon_5 = 6.5$.

response of a five-layer Fabry–Perot filter and report the results for our design solution in Fig. 5. The design curve was obtained [18] with a forward-scattering approach for a five-layer structure with thicknesses from bottom to top of 0.2, 0.5, 0.22, 0.5, and 0.2 cm. The correspondent original dielectric constants of the five materials were 6.13, 1, 6.13, 1, and 6.13. For use with our inverse approach, the design curve was approximated according to (10) and its rational representation was obtained numerically for $N = 2$ and $K = 1$ using five wavelengths unequally distributed in the design range, specifically at 1.8, 1.9, 1.95, 1.986, and 2.1 cm. The "cell periodicity" was taken to be 0.1 cm and the overall thickness was fixed at 1.62 cm. Note that the solution found by the GA is symmetric with values of thicknesses and dielectric constants very close to those used to generate the design curve. In particular, no symmetry requirements were introduced as constraints. Since the reconstructed transmittivity is in very good agreement with the prescribed one, we can see that the sensitivity of the response to small variations in the design parameters (thicknesses and dielectric constants) is very small. This property is well known for Fabry–Perot filters. We note that while we are not advocating the use of our design approach for Fabry–Perot structures, we chose this example for validation of our technique, showing that starting from the response of a Fabry–Perot filter, the algorithm finds a solution in this class.

VI. Conclusion

The feasibility of novel all-dielectric waveguide grating filters has been demonstrated using a GA to optimize material dielectric constants and placement of geometric boundaries separating homogeneous regions of the periodic cell. Exploiting the GA's ability to sample a specified parameter space globally, we show the existence of simple filter geometries (not previously reported) utilizing a small number of layers and/or gratings and yielding bandpass or stopband responses with user defined linewidth. Novel solutions are illustrated for a very narrowband (Lorentzian) single grating transmission filter and a relatively broad-band double grating reflection filter. We believe that our three-material single-grating structure achieving narrow-transmission linewidth, symmetric response, and very low sidebands has not been demonstrated before. An efficient implementation is presented where the most expensive part of the computation is reduced by: 1) conveniently filling a set of impedance matrices associated with a MoM discretization and 2) explicitly solving the MoM only at a small number of design frequencies/illumination angles and then extrapolating the solution for the (normally) much larger set of design frequencies/illumination angles of interest. Thanks to these features, the availability of a parallel GA library and a supercomputer we were able to obtain design solutions in about two hours using a Cray T3D. The general approach outlined in this paper, combining an efficient forward scattering module with a GA-based inversion scheme, can be applied to other electromagnetic system design problems.

Appendix

Applying Kumar's transformation to (4) it is obtained

$$\begin{aligned} E^s(x,z) &= \frac{-\omega\mu}{4}\int_0^{t(x)} dz' \int_0^{T_x} dx'\, J(x',z') \\ &\quad \times \sum_m \Big[H_0^{(2)}\big(k\sqrt{(x-x'-mT_x)^2+(z-z')^2}\big) - H_0^{(2)} \\ &\quad \times \big(k\sqrt{(x-x'-mT_x)^2+(|z-z'|+\delta)^2}\big)\, e^{+jk_{x_0}mT_x}\Big] \\ &\quad - \frac{\omega\mu}{4}\int_0^{t(x)} dz' \int_0^{T_x} dx'\, J(x',z') \sum_m H_0^{(2)} \\ &\quad \times \big(k\sqrt{(x-x'-mT_x)^2+(|z-z'|+\delta)^2}\big)\, e^{+jk_{x_0}mT_x} \end{aligned} \tag{A.1}$$

where δ is the shift away from the $|z - z'|$ axis. The first integral contains an integrable singularity, while the second can be transformed into a quickly convergent summation. Use

is made of the Poisson sum formula to convert the second integral in (A.1) to a spectral domain summation. The Poisson sum formula is

$$\sum_{m=-\infty}^{\infty} f(\alpha m) = \frac{1}{\alpha} \sum_{m=-\infty}^{\infty} F\left(\frac{2m\pi}{\alpha}\right)$$
$$F(\omega) = \int_{-\infty}^{\infty} e^{j\omega z} f(z)\, dz$$

where we take

$$f(mT_x) = H_0^{(2)}\left(k\sqrt{(x-x'-mT_x)^2 + (|z-z'|+\delta)^2}\right) e^{jk_{x_0}mT_x}$$

and

$$F(k_x) = \frac{1}{2jk_z} e^{j(k_x+k_{x_0})(x-x')} e^{-jk_z(|z-z'|+\delta)}.$$

The summation in the second integral of (A.1) becomes

$$\frac{1}{T_x} \sum_{m=-\infty}^{\infty} \frac{1}{2jk_{z_m}} e^{j(\frac{2\pi m}{T_x}+k_{x_0})(x-x')} e^{-jk_{z_m}(|z-z'|+\delta)}$$

and the second integral is reduced to

$$\frac{\omega}{4} \sum_m \frac{1}{2jk_{z_m}} \Psi_m(x) \int_0^{t(x)} dz'\, \tilde{J}_m(z')\, e^{-jk_{z_m}(|z-z'|+\delta)}. \tag{A.2}$$

Then (A.1) is given by

$$E^s(x,z) = \int_0^{T_x} dx' \int_0^t dz'\, J(x',z') \left[Z_m^p(x,z \mid x',z') - Z_m^p(x,z \mid x',z'+\delta)\right] + \sum \tilde{Z}_m\, \tilde{J}_m^{\pm} \Psi_m(x)\, e^{\mp jk_{z_m}(z+\delta)} \tag{A.3}$$

where the $-$ sign applies for $z > z'$ and the $+$ sign for $z < z'$. The first integral in (A.3) is the contribution from the singularity, whereas the summation pertains to the nonsingular part

$$\tilde{J}_m^t = \int_0^{T_x} dx' \int_0^{t(x)} dz'\, J(x',z') \Psi_m^*(x')\, e^{\pm jk_{z_m}z'}$$
$$\tilde{Z}_m = -\frac{\omega\mu}{8jk_{z_m}}$$
$$Z_m^p(x,z \mid x',z') = \frac{-\omega\mu}{4} \sum_m H_0^{(2)}(x,z \mid x',z')\, e^{jk_{x_0}mT_x}.$$

ACKNOWLEDGMENT

The authors would like to thank Dr. D. Levine, formerly with Argonne National Laboratory, Argonne, IL, and presently with the Boeing Company, Seattle, WA, for discussions on and assistance with use of PGAPACK. They would also like to thank S. Tibuleac, University of Texas at Arlington, for discussions on dielectric waveguide gratings filters and for providing independent calculations and verifications of some of the results presented here. In addition, use of the Cray Supercomputers at the Jet Propulsion Laboratory, Pasadena, CA, is acknowledged.

REFERENCES

[1] T. M. Habashy, L. M. Oristaglio, and A. T. de Hoop, "Simultaneous non linear reconstruction of two-dimensional permittivity and conductivity," *Radio Sci.*, vol. 29, pp. 1101–1118, Aug. 1994.
[2] R. E. Kleinman and P. M. van de Berg, "Two-dimensional location and shape reconstruction," *Radio Sci.*, vol. 29, pp. 1157–1169, Aug. 1994.
[3] D. Levine, "Users guide to the PGAPACK parallel genetic algorithm library," Argonne Nat. Lab. 95/18, Jan. 1996.
[4] R. L. Haupt, "Thinned arrays using genetic algorithms," *IEEE Trans. Antennas Propagat.*, vol. 42, pp. 993–999, July 1994.
[5] E. Michielssen, J.-M. Sajer, S. Ranjithan, and R. Mittra, "Design of lightweight, broad-band microwave absorbers using genetic algorithms," *IEEE Trans. Antennas Propagat.*, vol. 41, pp. 1024–1030, June 1993.
[6] T. Eisenhammer, M. Lazarov, M. Leutbecher, U. Schoffel, and R. Sizmann, "Optimization of interference filters with genetic algorithms applied to silver-based heat mirrors," *Appl. Opt.*, vol. 32, pp. 6310–6315, Nov. 1993.
[7] A. Boag, A. Boag, E. Michielssen, and R. Mittra, "Design of electrically loaded wire antennas using genetic algorithms," *IEEE Trans. Antennas Propagat.*, vol. 44, pp. 687–695, May 1996.
[8] E. E. Altshuler and D. S. Linden, "Design of a loaded monopole having hemispherical coverage using genetic algorithms," *IEEE Trans. Antennas Propagat.*, vol. 45, pp. 1–4, Jan. 1997.
[9] A. John and R. H. Jansen, "Evolutionary generation of (M)MIC component shapes using 2.5D EM simulation and discrete genetic optimization," in *IEEE MTT-S Dig.*, 1996, vol. 44, pp. 745–747.
[10] S. Chakrabarti, K. R. Demarest, and E. K. Miller, "An extended frequency-domain Prony's method for transfer function parameter estimation," *Int. J. Numer. Modeling: Electron. Networks, Devices, Fields*, vol. 6, pp. 269–281, 1993.
[11] N. Amitay, V. Galindo, and C. Wu, *Theory and Analysis of Phased Array Antennas.* New York: Wiley, 1972, pp. 310–313.
[12] R. Jorgenson and R. Mittra, "Efficient calculation of the free-space periodic green's function," *IEEE Trans. Antennas Propagat.*, vol. 38, pp. 633–642, May 1990.
[13] D. E. Goldberg, *Genetic Algorithms*. New York: Addison-Wesley, 1989.
[14] Z. Michalewicz, *Genetic Algorithms + Data Structures = Evolution Programs.* New York: Springer-Verlag, 1992, pp. 75–82.
[15] S. S. Wang and R. Magnusson, "Multilayer waveguide-grating filters," *Appl. Opt.*, vol. 34, pp. 2414–2420, May 1995.
[16] R. Magnusson and S. S. Wang, "Transmission bandpass guided-mode resonance filters," *Appl. Opt.*, vol. 34, pp. 8106–8109, Dec. 1995.
[17] R. Magnusson, S. S. Wang, T. D. Black, and A. Sohn, "Resonance properties of dielectric waveguide gratings: Theory and experiments at 4–18 GHz," *IEEE Trans. Antennas Propagat.*, vol. 42, pp. 567–569, Apr. 1994.
[18] S. Tibuleac, Univ. Texas at Arlington, private communication, Dec. 1996.

Cinzia Zuffada (SM'90), for photograph and biography, see p. 459 of the April 1996 issue of this TRANSACTIONS.

Tom Cwik (S'79–M'86–SM'94), for photograph and biography, see p. 459 of the April 1996 issue of this TRANSACTIONS.

Christopher Ditchman, photograph and biography not available at the time of publication.